Monitoring induced distributed double-couple sources using Marchenko-based virtual receivers

Joeri Brackenhoff, Jan Thorbecke and Kees Wapenaar

January 13, 2019

Abstract

Forecasting induced seismicity responses for field data is difficult if no detailed model of the subsurface is available, which generally is the case. As an alternative, reflection data of the subsurface and a non-detailed background model can be used in the Marchenko method to obtain virtual receivers in the subsurface. By employing homogeneous Green's function retrieval, the responses between the virtual receivers are obtained. This approach is applied to synthetic data and a double-couple signature is imposed on the response, to simulate a small-scale induced seismicity response. To simulate a large-scale response, several small-scale responses are superposed. These methods are applied to a field dataset as well to forecast a small-scale and large-scale induced seismicity response.

Introduction

The study of induced seismicity signals is challenging due to the complex nature of the signals, which makes it hard to properly process these signals (McClellan et al., 2018). Studies into the modeling of signals can take into account a great deal of these complex effects (Cruz-Atienza and Virieux, 2004), however, they require a detailed model, which is generally not available. The study of forecasting induced seismicity signals in the subsurface and at the surface of the Earth can be improved through the use of virtual receivers, which are receivers that are not physically present in the subsurface, rather, they are created from measurements at physical receivers at the surface. These virtual receivers can be created through use of the Marchenko method (Wapenaar et al., 2014; Slob et al., 2014), which requires reflection data at the surface of the Earth and an estimation of the first arrival from the virtual receiver location to the surface of the Earth. The first arrival can be estimated from a background velocity model. Assuming that these types of data are available, a dense network of virtual receivers can be created in the subsurface, without the use of an exact model. By applying homogeneous Green's function retrieval, the responses between these virtual receiver locations can be obtained. The classical representation for this retrieval requires receivers on a boundary enclosing the virtual receiver locations (Porter, 1970), however in recent years a single-sided representation has been introduced that works with receivers that are only located at a single-sided open boundary (Wapenaar et al., 2016).
By applying the Marchenko method and homogeneous Green's function retrieval, we model a small-scale induced seismicity response in the subsurface from only reflection data at the surface, without an exact model. By superposing several responses from individual small-scale (monopole or double-couple) sources together, we create a more complex signal that represents a large rupture plane. We validate these results on synthetic data and then apply the same approach on field data to forecast possible induced seismicity events, which normally would not be possible as no exact model is available for these data.

Theory

We make use of the Green's function $G(\mathbf{x},\mathbf{x}_B,t)$, which is the response of a medium at location $\mathbf{x}$ at time t to an impulsive point source at location $\mathbf{x}_B$, where $\mathbf{x}=(x_1,x_2,x_3)$ is the cartesian coordinate vector. Also, we use the homogeneous Green's function $G_\mathrm{h}=G_\mathrm{h}(\mathbf{x},\mathbf{x}_B,t)$, a superposition of the Green's function with its time reversal, $G(\mathbf{x},\mathbf{x}_B,-t)$, that obeys the homogeneous wave equation,

$$\partial_i\left(\frac{1}{\rho(\mathbf{x})}\partial_i G_\mathrm{h}\right)-\kappa(\mathbf{x})\partial_t^2 G_\mathrm{h}=0, \tag{1}$$

where $\rho(\mathbf{x})$ is the density and $\kappa(\mathbf{x})$ the compressibility of the medium, ∂_t the temporal partial differential operator $\frac{\partial}{\partial t}$ and ∂_i a component of a vector containing the spatial partial differential operators in the three principal directions $\left(\frac{\partial}{\partial x_1},\frac{\partial}{\partial x_2},\frac{\partial}{\partial x_3}\right)$.
The homogeneous Green's function is obtained through the application of the single-sided homogeneous Green's function representation in the frequency domain (Wapenaar et al., 2016):

$$G_\mathrm{h}(\mathbf{x}_A,\mathbf{x}_B,\omega)=4\Re\int_{\mathbb{S}_0}\frac{1}{i\omega\rho(\mathbf{x})}G(\mathbf{x},\mathbf{x}_B,\omega)\partial_3\left(f_1^+(\mathbf{x},\mathbf{x}_A,\omega)-\{f_1^-(\mathbf{x},\mathbf{x}_A,\omega)\}^*\right)\mathrm{d}\mathbf{x}, \tag{2}$$

where $f_1^+(\mathbf{x},\mathbf{x}_A,\omega)$ is the downgoing and $f_1^-(\mathbf{x},\mathbf{x}_A,\omega)$ the upgoing part of a focusing function that focuses to a focal location $\mathbf{x}_A$ in the subsurface, i is the imaginary unit, ω the angular frequency, $\Re$ denotes the real part of a complex function and $\mathbb{S}_0$ is the single-sided surface of the Earth over which the integral is evaluated. The source location of the Green's function in equation (2) will become the virtual source location of the new signal and the focal location of the focusing function will become the virtual receiver location. The Green's function and focusing function that are required for this application are obtained through the use of the Marchenko method, the details of which can be found in Wapenaar et al. (2014) and Slob et al. (2014).
Equation (2) obtains the homogeneous Green's function for a single location in the subsurface, however, in case of an extended rupture plane, the signal originates from a larger area. By applying equation (2)

for multiple locations, the extended signal can be constructed,

$$P(\mathbf{x}_A,t) = \sum_{k=1}^{N} H(t-t^{(k)})G_{\mathrm{h}}(\mathbf{x}_A,\mathbf{x}_B^{(k)},t-t^{(k)}), \tag{3}$$

where $P(\mathbf{x}_A,t)$ is the response from a large-scale induced seismicity source, $H(t-t^{(k)})$ a Heaviside step function, $\mathbf{x}_B^{(k)}$ the k-th virtual source location in the subsurface and $t^{(k)}$ a time shift for each individual homogeneous Green's function. Equation (3) takes the homogeneous Green's functions obtained through equation (2), isolates the causal part of the homogeneous Green's function and shifts this signal in time before all the shifted causal parts are superposed. This resulting signal simulates a signal that originates from a fault over a longer period of time.

Results

We make use of the data shown in Figure 1. Figure 1-(a) and (b) show a synthetic density and velocity model, respectively, that are used to model an acoustic reflection response. An example of a common-source record of this reflection response is shown in Figure 1-(d). The velocity model in Figure 1-(b) is smoothed and used with a homogeneous density model to estimate the first arrivals from the subsurface locations to the surface of the model. These first arrivals and the reflection response are the only input for the Marchenko method.

Using the acoustic Marchenko method, the required focusing functions and Green's functions are

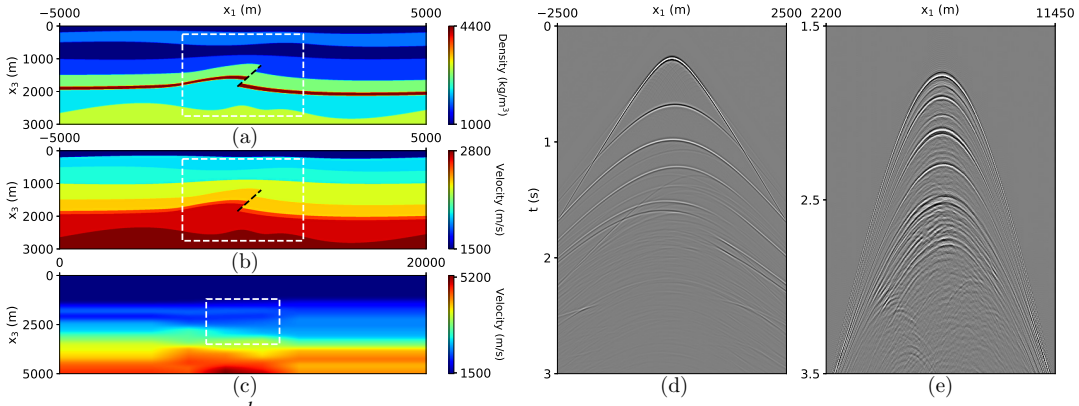

Figure 1: (a) Density in $\frac{kg}{m^3}$ and (b) velocity in $\frac{m}{s}$ of the synthetic data. The white boxes indicate the locations of the snapshots from Figure 2 and 3. The black dashed line indicates the location of a fault plane. (c) Velocity in $\frac{m}{s}$ of the subsurface in the Vøring basin. The white box indicates the locations of the snapshots from Figure 4. (d) Common-source record of the modeled acoustic data using the models from (a) and (b). (e) Common-source record of the field data from the Vøring basin.

retrieved for the application of the representation in equation (2). The area of interest is denoted with a white box in Figure 1-(a) and (b). For each location in this area a focusing function is retrieved to act as a virtual receiver location. One Green's function is retrieved as well to acts as a virtual source. Additionally, a double-couple signature inclined at 45 degrees is imposed to this response, to represent a small-scale induced seismicity response (Aki and Richards, 2002). Snapshots of the homogeneous Green's function that is obtained using these functions in equation (2) are shown in Figure 2-(e)-(h). The source location of the homogeneous Green's function is well defined and the scattering of the wavefield takes place along the geological layer interfaces. For a comparison of the arrival times, we modeled the response to a monopole point source for the same area in the subsurface. Snapshots of this response are shown in Figure 2-(a)-(d). When comparing the homogeneous Green's function to the modeling, the match between the source location, the presence and arrival times of the events is strong. Some high-angle parts of the events are not present for the homogeneous Green's function, due to the fact that these angles are not recorded in the reflection response.

To forecast a larger scale induced seismicity response, we use the same focusing functions as for the previous approach, however, more than one Green's function is retrieved. The source locations of the Green's functions are placed along the fault plane, indicated with the black dashed line in Figure 1-(a) and (b). The orientation of the fault plane is 45 degrees, so the signature of the Green's functions are

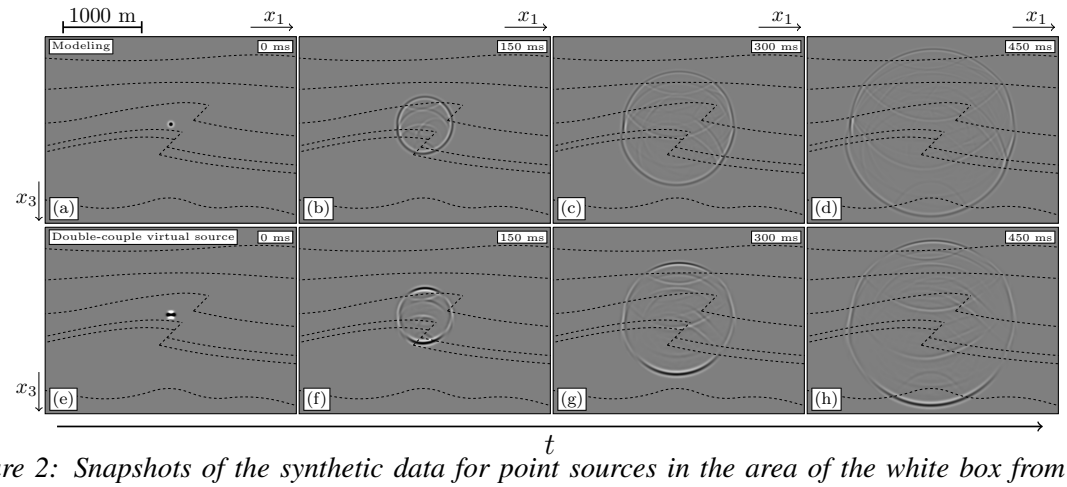

Figure 2: Snapshots of the synthetic data for point sources in the area of the white box from Figure 1-(a) and (b). (a)-(d) snapshots of the wavefield for a modeled response to a monopole source. (e)-(h) snapshots of the wavefield for a retrieved homogeneous Green's function using equation (2) *for a double-couple point source inclined at 45 degrees. The black dashed lines indicate the locations of geological layer interfaces.*

set to a double-couple signature at the same inclination. Several homogeneous Green's function are obtained through the use of equation (2). Equation (3) is then used to isolate the causal parts of these signals, shift them in time and superpose them. To simulate the heterogeneous nature of a fault plane, a random amplitude is assigned to each homogeneous Green's function. The snapshots of the result are shown in Figure 3-(e)-(h). Similar to the result for the small-scale response, the scattering of the wavefield takes place along the geological layer interfaces. The source is now no longer a single point, rather it evolves over time along the fault plane. The propagation of the source along the fault is clear. Also, the wavefield responses for these source locations using monopole sources with the same random amplitude scaling were modeled. The snapshots of the result are shown in Figure 3-(a)-(d). The match between the source location, presence and arrival times of the events is of similar quality as for the small-scale response.

To show that our approach works on field data, we applied the method to a dataset from the Vøring

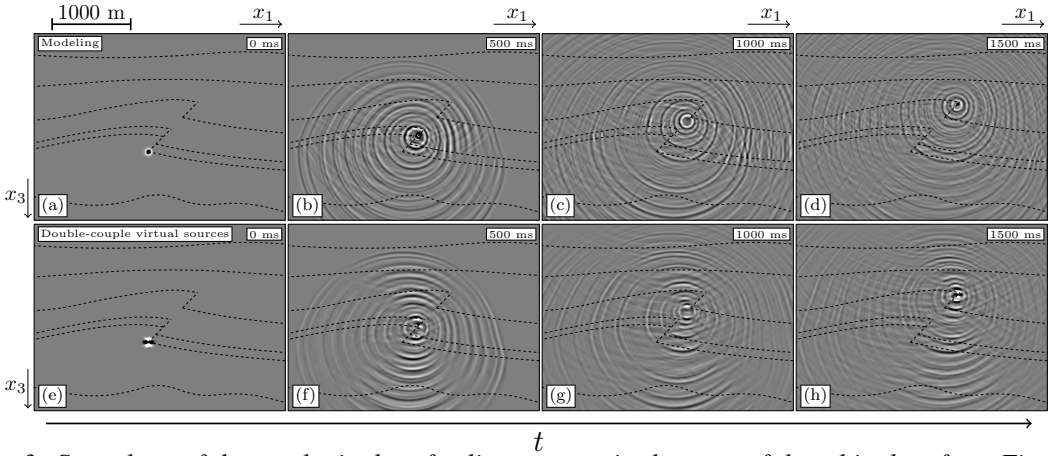

Figure 3: Snapshots of the synthetic data for line sources in the area of the white box from Figure 1-(a) and (b). (a)-(d) snapshots of the wavefield for a modeled response to a series of monopole point sources. (e)-(h) snapshots of the wavefield for a series retrieved homogeneous Green's functions with random amplitudes using equation (3) *for double-couple point sources inclined at 45 degrees. The black dashed lines indicate the locations of geological layer interfaces.*

basin, which was supplied by Equinor. An example of a common-source record is shown in Figure 1-(e) and the accompying smooth velocity model is shown in Figure 1-(c), where the area of interest for the retrieval of the response is indicated with a white box. These data are the only types of input for the Marchenko method. We perform the retrieval for a small-scale induced seismicity response, similar to the results in Figure 2, and for the large-scale induced seismicity response, similar to the results in Figure 3. Snapshots of the result for the small-scale response using a double-couple signature inclined at -20 degrees are shown in Figure 4-(a)-(d) and snapshots of the result for the large-scale response using a

double-couple signature inclined with the fault at 67 degrees are shown in Figure 4-(e)-(h). No modeling can be performed for this area, as no exact model is available. To make an estimation of the accuracy, an image of the subsurface is independently constructed and used as an overlay. The scattering of the wavefield takes place along the location of the interfaces that are present in the image, while the source locations are well defined and propagate along the fault plane, which is indicated with the red dashed line.

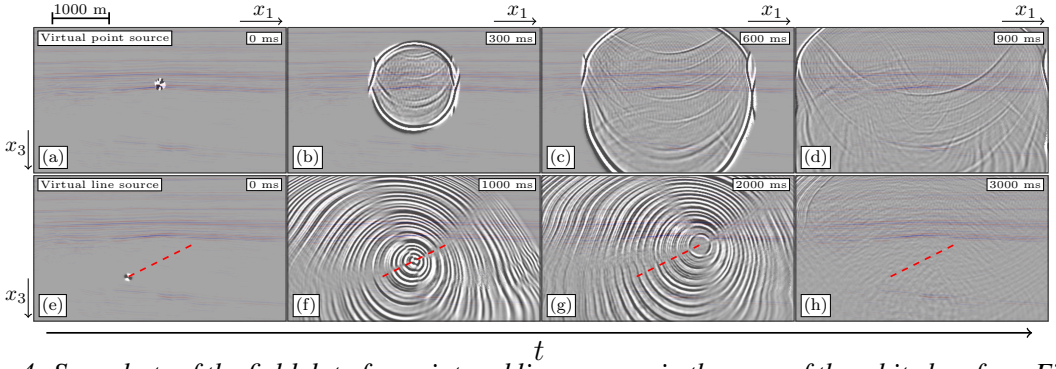

Figure 4: Snapshots of the field data for point and line sources in the area of the white box from Figure 1-(c). (a)-(d) snapshots of the wavefield for a retrieved homogeneous Green's function using equation (2) *for a double-couple point source inclined at -20 degrees. (e)-(h) snapshots of the wavefield for a series of retrieved homogeneous Green's functions with random amplitudes using equation* (3) *for double-couple point sources inclined at 67 degrees. The red line indicates the location of the simulated fault plane. All snapshots contain an overlay of an independently constructed image of the subsurface.*

Conclusions

We have shown that we can forecast both small-scale and large-scale induced seismicity responses, using only single-sided reflection data and no exact model. The results on the synthetic data were validated using the information from an exact model and modeling of the wavefield response. The approach was then used on field data to forecast a possible small-scale and large-scale induced seismicity response. The result shows a similar quality to what was achieved on the synthetic data.

Acknowledgements

This work has received funding from the European Union's Horizon 2020 research and innovation programme: European Research Council (grant agreement 742703). The authors thank Equinor ASA for giving permission to use the vintage seismic reflection data of the Vøring Basin and Eric Verschuur and Jan-Willem Vrolijk for their assistance with the processing of the vintage seismic reflection data.

References

Aki, K. and Richards, P.G. [2002] Quantitative seismology.

Cruz-Atienza, V. and Virieux, J. [2004] Dynamic rupture simulation of non-planar faults with a finite-difference approach. Geophysical Journal International, **158**(3), 939–954.

McClellan, J.H., Eisner, L., Liu, E., Iqbal, N., Al-Shuhail, A.A. and Kaka, S.I. [2018] Array processing in microseismic monitoring: Detection, enhancement, and localization of induced seismicity. IEEE Signal Processing Magazine, **35**(2), 99–111.

Porter, R.P. [1970] Diffraction-limited, scalar image formation with holograms of arbitrary shape. Journal of the Optical Society of America, **60**(8), 1051–1059.

Slob, E., Wapenaar, K., Broggini, F. and Snieder, R. [2014] Seismic reflector imaging using internal multiples with Marchenko-type equations. Geophysics, **79**(2), S63–S76.

Wapenaar, K., Thorbecke, J., van Der Neut, J., Broggini, F., Slob, E. and Snieder, R. [2014] Marchenko imaging. Geophysics, **79**(3), WA39–WA57.

Wapenaar, K., Thorbecke, J. and van der Neut, J. [2016] A single-sided homogeneous Green's function representation for holographic imaging, inverse scattering, time-reversal acoustics and interferometric Green's function retrieval. Geophysical Journal International, **205**(1), 531–535.